

# Quantized Anomalous Hall Effect in Two-Dimensional Ferromagnets - Quantum Hall Effect from Metal -

Masaru Onoda<sup>1\*</sup> and Naoto Nagaosa<sup>1,2†</sup>

<sup>1</sup>*Correlated Electron Research Center (CERC), National Institute of Advanced*

*Industrial Science and Technology (AIST), Tsukuba Central 4, Tsukuba 305-8562, Japan*

<sup>2</sup>*Department of Applied Physics, University of Tokyo, Bunkyo-ku, Tokyo 113-8656, Japan*

(Dated: November 2, 2018)

We study the effect of disorder on the anomalous Hall effect (AHE) in two-dimensional ferromagnets. The topological nature of AHE leads to the integer quantum Hall effect from a metal, i.e., the quantization of  $\sigma_{xy}$  induced by the localization except for the few extended states carrying Chern number. Extensive numerical study on a model reveals that Pruisken's two-parameter scaling theory holds even when the system has no gap with the overlapping multibands and without the uniform magnetic field. Therefore the condition for the quantized AHE is given only by the Hall conductivity  $\sigma_{xy}$  without the quantum correction, i.e.,  $|\sigma_{xy}| > e^2/(2h)$ .

PACS numbers: 72.15.Rn, 73.43.-f, 75.47.-m, 75.70.-i

The origin of the anomalous Hall effect (AHE) has been a subject of extensive controversy for a long term. One is based on the band picture with the relativistic spin-orbit interaction [1], while the other is due to the impurity scatterings [2]. Most of the succeeding theories follows the idea that the AHE occurs due to the scattering events modified by the spin-orbit interaction, i.e., the skew scattering or the side jump mechanism [3]. Recently several authors recognized the topological nature of the AHE discussed in Refs. [4, 5, 6]. In this formalism, the Hall conductivity  $\sigma_{xy}$  is given by the Berry phase curvature in the momentum ( $\vec{k}$ -) space integrated over the occupied states [7]. Also there appeared some experimental evidences supporting it [8]. Therefore it is very important to study the effect of the scatterings by disorder, which makes  $\vec{k}$  ill-defined, to see the topological stability of this mechanism for AHE.

This issue is closely related to the integer quantum Hall effect (IQHE) [9] but there are several essential differences. Usually the topological stability which guarantees the quantization of some physical quantity, e.g.,  $\sigma_{xy}$ , has been discussed in the context of the adiabatic continuation [9]. Therefore it appears that the gaps between Landau levels in pure system are needed to start with even though the disorder potential eventually buries it. In the IQHE system without disorder, the periodic potential is irrelevant because the carrier concentration is much smaller than unity per atom. Although numerical simulations [10] use lattice models, the main concern is put on the limit of dispersionless Landau levels separated by the gaps. In the present case, i.e., in ferromagnetic metals, there are multiple bands overlapping without the gaps in the density of states. The periodicity of the lattice remains unchanged, which prohibits the uniform magnetic field and also gives a large energy dispersion. In

the language of the effective magnetic field for electrons, it reaches a huge value of the order of  $\sim 10^4$  Tesla, i.e., the magnetic cyclotron length is of the order of the lattice constant, but the net flux is zero when averaged over the unit cell. Therefore these two cases belong to quite different limits although the symmetries of the systems are common, i.e., the unitary class without time-reversal nor spin-rotational symmetry

In this paper we report on an extensive numerical study on two-dimensional (2D) models of AHE including the disorder potentials. It is found that the topological nature of AHE leads to a dramatic phenomenon, i.e., the ferromagnetic metal turns into an integer quantized Hall system by introducing disorder. This is due to the topological stability of the Chern numbers carried by the extended states which are energetically separated by the continuum of the localized states inbetween. Namely the localized state can not have a finite Chern number, and the integer topological number can not change smoothly, i.e., it jumps when it changes. These two facts leads to the protection of the extended state carrying a Chern number against the weak disorder. The finite-size scaling analysis is compatible with the two-parameter RG theory of Pruisken [11], which predicts the plateau transition at  $|\sigma_{xy}| = 0.5e^2/h$ . The critical exponents are consistent with that of the IQHE. This problem is not an academic one; the recent technology can fabricate very fine thin films of ferromagnetic metals with large enough single domain. When the coherent length of such a thin film is longer than the thickness, it can be regarded as a multi-channel 2D system. These systems can offer a possible laboratory to test our theory.

The essence of the AHE is that the Berry phase of the Bloch electron is induced by the spin-orbit interaction in the presence of the magnetization, which is modeled by the complex transfer integrals [5]. Each band often gains finite Chern number even though the density of states has no gap. The minimal model describing this situation is that proposed by Haldane [12] and its extension. This model is defined on a honeycomb lattice

\*Electronic address: m.onoda@aist.go.jp

†Electronic address: nagaosa@appi.t.u-tokyo.ac.jp

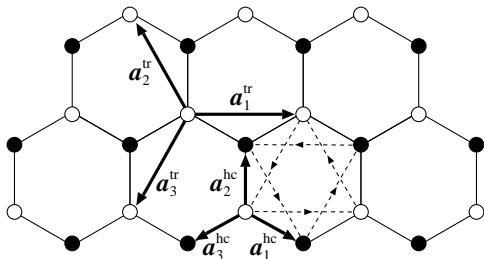


FIG. 1: Haldane's model defined on honeycomb lattice [12]. Open and closed circles represent the  $A$  and  $B$  sublattice sites respectively. The thick arrows  $\vec{a}_{1,2,3}^{\text{hc}}$  and  $\vec{a}_{1,2,3}^{\text{tr}}$  are the lattice vectors of honeycomb lattice and those of triangle sublattice respectively. The dashed lines represent next-nearest neighbor hopping.

containing two atoms in a unit cell (Fig. 1). Using the Fourier transformation  $\mathbf{c}_k^\dagger = (c_{A\vec{k}}^\dagger, c_{B\vec{k}}^\dagger)$  of the spinor representation  $(c_{\vec{r} \in A}^\dagger, c_{\vec{r} \in B}^\dagger)$ , its Hamiltonian is written as  $H = \sum_{\vec{k}} \mathbf{c}_k^\dagger \mathcal{H}_{\vec{k}} \mathbf{c}_k$ , where

$$\begin{aligned} \mathcal{H}_{\vec{k}} = & 2t_1 \cos \phi \sum_{i=1,2,3} \cos(\vec{k} \cdot \vec{a}_i^{\text{tr}}) \tau^0 \\ & + t_0 \sum_i \left[ \cos(\vec{k} \cdot \vec{a}_i^{\text{hc}}) \tau^1 - \sin(\vec{k} \cdot \vec{a}_i^{\text{hc}}) \tau^2 \right] \\ & + \left[ m + 2t_1 \sin \phi \sum_i \sin(\vec{k} \cdot \vec{a}_i^{\text{tr}}) \right] \tau^3. \end{aligned} \quad (1)$$

$\tau^0$  is the unit matrix and  $\tau^{1,2,3}$  are the Pauli matrices. Here we assume the perfect spin-polarization and use the spinless fermions. The complex next-nearest neighbor hopping integral  $t_1 e^{i\phi}$  is introduced in addition to the real one  $t_0$  between the nearest neighbors.  $\vec{a}_{1,2,3}^{\text{tr}}$  are the lattice vectors of triangle sub-lattice, while  $\vec{a}_{1,2,3}^{\text{hc}}$  are those of honeycomb lattice.

The extended model is given by adding another layer with the change  $t_1 \rightarrow -t_1$  to the original single-layer model given above. Furthermore we introduce the energy difference between the layers by shifting the uniform potential  $\pm u$ . Then the extended model has the symmetric and gapless density of states in contrast to the original one. In Figs. 2 are shown the density of states and  $\sigma_{xy}$  for the single-layer (a) and double-layer (b) models, respectively. In the single-layer case,  $\sigma_{xy}$  is quantized to be  $e^2/h$  when the Fermi energy lies within the gap, while it is not in the double-layer case where the gap collapses.

Now we introduce the on-site disorder potential to the single-layer model, which is randomly distributed in the range  $[-W/2, W/2]$ , and study the localization problem in terms of the transfer matrix method [13]. Figure 3(a) shows the dependence of the renormalized localization length  $\lambda_M/(2M)$  of a quasi-1D tube with  $2M$ -sites circumference on the strength of disorder potential  $W$ . In each figure, the lines for  $M = 4, 8, 16, 32$  are plotted. We

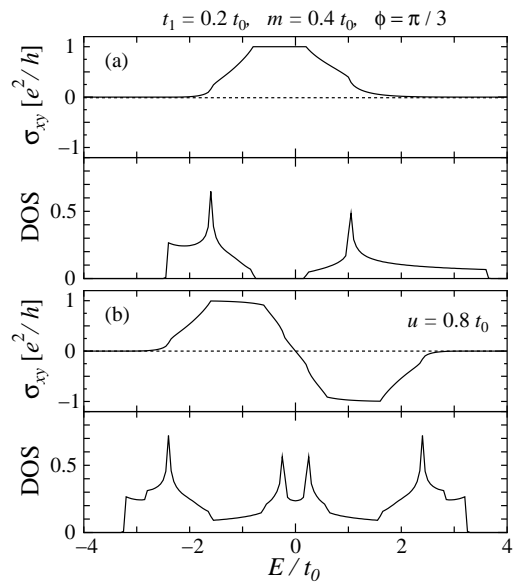


FIG. 2: Hall conductivity  $\sigma_{xy}$  and the density of states for the pure single-layer model with  $t_1 = 0.2t_0$ ,  $m = 0.4t_0$  and  $\phi = \pi/3$  (a), and for the pure double-layer model with  $t_1 = 0.2t_0$ ,  $m = 0.4t_0$ ,  $u = 0.8t_0$  and  $\phi = \pi/3$  (b).

have also calculated up to the system size  $M = 64$  around the lower extended state. (These additional data are used in the analyses for the localization length and its critical exponent.) The length of a tube is typically  $\sim 10^5$  sites and the accuracy of data is within a few percent. We can see that extended states are isolated in energy. They merge with each other at a critical value  $6 < W_c < 7$ , and disappear, i.e., all states are localized. This behavior is the same as that observed in the ordinary IQH system on a square lattice with external magnetic field [10]. It is noted that the pair annihilation of extended states always occurs between those with the opposite Chern numbers [10]. Actually, two extended states in Fig. 3 originate from lower and upper bands which have opposite Chern numbers,  $\pm 1$ , respectively.

Next we analyze the data to obtain a characteristic length  $\xi(E, W)$ , which depends on  $E$  and  $W$  but not on  $M$ , by the scaling hypothesis,  $\lambda_M(E, W)/M = f(\xi(E, W)/M)$ , where  $f(x)$  is a scaling function [14]. As for a localized state,  $\xi(E, W)$  is interpreted as its localization length in the thermodynamic limit. Figure 3(c) shows  $\xi(E, W = 5.0t_0)$  around the lower extended state at  $E = E_c$ . From this data, the critical exponent  $\nu$  ( $\xi \propto |E - E_c|^{-\nu}$ ) is estimated as  $\nu = 2.37 \pm 0.05$  with  $E_c = (-0.69 \pm 0.01)t_0$ . Figure 3(d) gives the log-log plot of the localization length  $\xi(E, 5.0t_0)$  as a function of the energy measured from  $E_c$ . The fitting is also shown as a solid line with the slope  $-\nu = -2.37$ . This value is in reasonable agreement with that estimated in the ordinary IQH system [15], e.g.  $\nu = 2.35 \pm 0.03$  [16].

The system-size dependence of  $\sigma_{xy}$  shown in Fig. 3(b) represents its scaling property. There are two critical

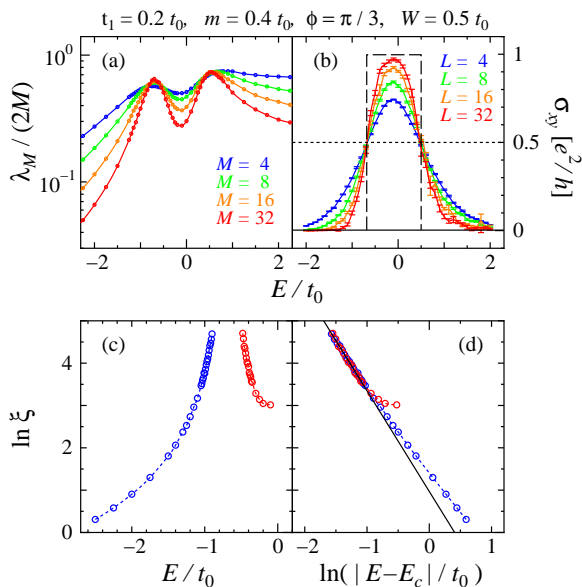


FIG. 3: (a) Localization length  $\lambda_M$  of a quasi-1D tube where  $M$  is the number of A(B) sites on the circumference.  $M = 4, 8, 16, 32$  are plotted. (b) System-size dependence of  $\sigma_{xy}$  in the single-layer system with  $2L \times 2L$  lattice points. The numbers of samples averaged are 81920, 20480, 5120, 1280 for  $L = 4, 8, 16, 32$  respectively. The errors are one standard deviation. (c) Log plot and (d) Log-log plot of Localization length  $\xi$  around the lower extended state at  $E_c = (-0.69 \pm 0.01)t_0$ . The solid line is a fitting result with the slope  $-\nu = -2.37$ .

points where there is no size dependence and which separate the two energy regions with the opposite size dependences.  $\sigma_{xy}$  at these critical points takes the value about  $0.5e^2/h$ . This is consistent with the analysis in terms of the effective field theory for the ordinary IQH system in the weak-localization region [11], and strongly suggests that the critical properties of this transition are same as those of the plateau transition  $\sigma_{xy} : 0 \leftrightarrow 1$ . The energy of these critical points coincide with that where the localization length diverges in Figs. 3(a) and (c). This means that the extended states with Chern number  $\pm 1$  exist there, and  $\sigma_{xy}$  in the thermodynamic limit ( $M \rightarrow \infty$ ) stays quantized to be  $e^2/h$  between these two energies [broken line in Fig. 3(b)].

Now we shall consider the double-layer model. The IQHE never occurs in this system with the above set of parameters unless the effect of disorder is taken into account. We consider the nontrivial case in which there are scattering events both within and between these layers. In this case, there is no gap between the initial and final states of the elastic scattering, and it is possible that all the states are localized once the disorder is introduced. However as shown below, the extended states and the Chern number carried by them are stable against the weak disorder. Here we define the strength of intra-layer scattering as  $W_0$  and represent the strength of inter-layer scattering by  $W_1$ . As seen in the upper panels of Fig. 4, there occur two energies, i.e.,  $E \cong -1.5t_0$  and  $E = 0$ ,

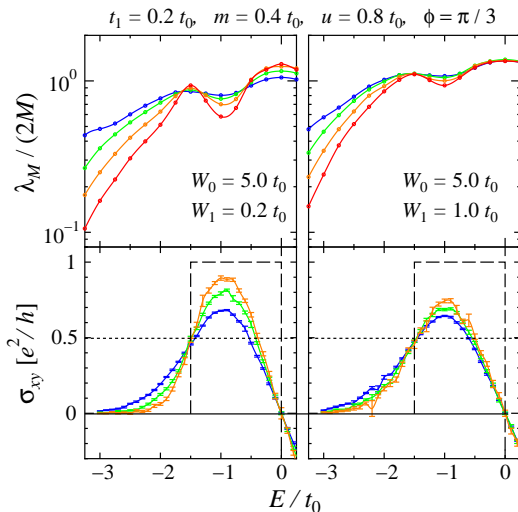


FIG. 4: Upper panels : the localization length  $\lambda_M$  of a quasi-1D tube where  $M$  is the number of A(B) sites on the circumference.  $M = 4, 8, 16, 32$  are plotted. Lower panels : the system-size dependence of  $\sigma_{xy}$  in the double-layer system with  $2L \times 2L$  lattice points. The numbers of samples averaged are 81920, 20480, 5120 for  $L = 4, 8, 16$  respectively. The color of each lines is for the same system-size as in Fig. 3(a) and (b).

at which  $\lambda_M/2M$  does not show  $M$ -dependence. This means that the extended states survives there as in Figs. 3 at least up to  $W_1 = 1.0t_0$ .

We next present the system-size dependence of  $\sigma_{xy}$ , as shown in the lower panels of Fig. 4. There appears two critical points for the transitions  $\sigma_{xy} : 0 \leftrightarrow 1$  and  $\sigma_{xy} : -1 \leftrightarrow 1$ . From the particle-hole symmetry,  $\sigma_{xy}(-E) = -\sigma_{xy}(E)$  is concluded. Therefore, there appear three critical points in the whole energy region. Because the single-layer model has at most two critical-points, the double-layer model could have maximum four. One may wonder why there appear only three critical-points in the present case. This is because the middle one is composed of two extended states which originally contribute to different critical points but carry the same Chern number, i.e.  $-1$ . These extended states merge (at least in the present numerical accuracy) but never pair-annihilate, because the composite of these extended states carry the non-zero Chern number  $-2$ . In other words, the conservation law of the topological charge prevents the localization.

$\sigma_{xy}$  at the lower critical-point takes the value  $\cong 0.5e^2/h$ . This value is again consistent with the analysis by Pruiskin and coworkers [11]. However,  $\sigma_{xy}$  at the middle critical-point is zero. This critical behavior seems to violate the prediction by the analysis in [11]. However, recent numerical studies for the ordinary IQH system reveals the new type of critical phenomena, i.e. the direct transitions  $\sigma_{xy} : 0 \leftrightarrow n$  ( $n > 1$ ) [10], which were experimentally observed in advance [17]. The critical property around the middle point is considered to belong to the same class as  $\sigma_{xy} : 0 \leftrightarrow 2$ . Although the

sample size is not large enough in the double-layer model, the size-dependence of  $\sigma_{xy}$  is consistent with the quantized plateau shown by the broken line in the lower panels of Fig. 4.

It is not difficult to generalize the non-linear sigma model approach for the localization problem to the case of multi-component model without time-reversal nor spin-rotational symmetry. This “*components*” means orbitals, spins, and channels in the multilayer cases altogether. This approach does not assume the finite gap at the starting. Following the derivation in Ref. [11], we obtain the Lagrangian:

$$L[\{Q_l\}] = - \sum_{l,l'} \frac{1}{2} [g^{-1}]_{ll'} \widetilde{\mathbf{Tr}} Q_l Q_{l'} + \mathbf{Tr} \ln \left[ E - \hat{H} + i\eta s + \sum_l iQ_l I_l \right], \quad (2)$$

where  $[g]_{ll'}$  is the scattering strength between components  $l$  and  $l'$ , and  $[I_l]_{ll'} = \delta_{ll'} \delta_{l'l}$ .  $\mathbf{Tr}$  ( $\ln$ ) is the trace (logarithm) of matrix with functional index ( $\vec{r}$ ) and discrete indices ( $p, a, l$ ), where  $p = \pm$  corresponds to the advanced and retarded fields respectively, and  $a$  runs over replicas.  $\widetilde{\mathbf{Tr}} O$  is the abbreviation for  $\int d\vec{r} \text{Tr} O(\vec{r})$  where  $O(\vec{r})$  is a matrix with  $p$  and  $a$  indices. The non-linear sigma model is the effective model for the massless Goldstone modes. In order to extract these modes, the parametrization  $Q_l = T_l P_l T_l^{-1}$  is useful. From the above Lagrangian, it is clear that inter-component scatterings  $[g^{-1}]_{ll'}$  ( $l \neq l'$ ) lock the out-of-phase modes  $T_l \neq T_{l'}$  ( $l \neq l'$ ), and therefore the effective model for massless in-phase modes, i.e.,  $T_l = T$ , reduces to the model identical to that in Ref. [11]. The coefficients of the stiffness and topological terms for these modes coincide with  $\sigma_{xx}$  and  $\sigma_{xy}$  respectively. It is noted that these  $\sigma_{xx}$  and  $\sigma_{xy}$  contain the contributions from all components, i.e., all orbitals, spins and channels. Then the scaling of  $\sigma_{xy}$  and  $\sigma_{xx}$  remains the same as given in Ref. [11]. This supports the finite-size scaling study given above.

In real systems, the Coulomb interaction can not be ne-

glected. In IQHE system, the  $\ln T$  dependence of  $\sigma_{xx}$  is observed [18] and is attributed to the quantum Coulomb correction [19]. However, the quantized  $\sigma_{xy}$  in the ground state is well described by the noninteracting electron model. The situation is similar here for the quantized AHE system. In the thin film of Fe,  $\ln T$ -dependence of  $\sigma_{xx}$  is observed while not for  $\sigma_{xy}$  [20], which is explained by the quantum Coulomb correction combined with the skew scattering mechanism [21].

Usually AHE is estimated by  $\rho_H \cong -\rho_{xx}^2 \sigma_{xy}$ , where  $\rho_H$ ,  $\rho_{xx}$  and  $\sigma_{xy}$  are measured as quantities in 3D. In good metals,  $\rho_{xx}$  is very small at low temperatures, and hence  $|\sigma_{xy}|$  is large although  $|\rho_H|$  is very small. Therefore it is possible that the quantized AHE is realized even in the conventional metallic ferromagnets such as Fe or Ni, when the thin film is fabricated. Actually, when we virtually consider thin film of  $n$ -layer systems, the 2D  $|\sigma_{xy}|$  at  $T_C/2$  is estimated as  $\sim 0.59ne^2/h$  for Fe [22],  $\sim 0.47ne^2/h$  for Ni [22], and  $\sim 0.20ne^2/h$  for SrRuO<sub>3</sub> (from the first article in Ref. [8]). Therefore, the condition  $|\sigma_{xy}| > 0.5e^2/h$  is not so difficult to achieve in the thin films of metallic ferromagnets. Extrapolating the  $\ln T$  behavior of  $\sigma_{xx}$  experimentally observed [20], the crossover temperature  $T_{\text{cross}}$  from weak to strong localization is estimated as  $T_{\text{cross}} \cong T_0 e^{-\frac{\sigma_0 h}{Ae^2}}$ , where  $T_0$  a reference temperature of the order of 10K,  $\sigma_0$  the Drude conductivity at  $T_0$ , and  $A$  is a sample-dependent scaling-exponent of the order of unity. Therefore, if the minimal  $\sigma_0 h / (Ae^2)$  is less than  $\sim 10$ , we have the chance to observe the quantized anomalous Hall effect in the experimentally realizable temperature. Considering that  $\sigma_{xy}$  have to be larger than  $0.5e^2/h$ , this condition means that the ratio  $\sigma_0 / \sigma_{xy}$  should be smaller than  $\sim 10$ . This novel quantized Hall state would prove the most dramatic consequence of the topological nature of the AHE.

The authors would like to thank Y. Tokura and A. Asamitsu for useful discussion. M. O. is supported by Domestic Research Fellowship from Japan Society for the Promotion of Science. N. N. is supported by the Ministry of Education, Science, Culture and Sports of Japan.

- 
- [1] R. Karplus and J. M. Luttinger, Phys. Rev. **95**, 1154 (1954); J. M. Luttinger, Phys. Rev. **112**, 739 (1958).  
[2] J. Smit, Physica **24**, 39 (1958).  
[3] J. Kondo, Prog. Theor. Phys. **27**, 772 (1962); P. Nozieres and C. Lewiner, J. Phys. (Paris) **34**, 901 (1973).  
[4] J. Ye *et al.*, Phys. Rev. Lett. **83**, 3737 (1999); S. H. Chun *et al.*, Phys. Rev. Lett. **84**, 757 (2000); K. Ohgushi *et al.*, Phys. Rev. B **62**, R6065 (2000); R. Shindou and N. Nagaosa, Phys. Rev. Lett. **87**, 116801 (2001).  
[5] M. Onoda and N. Nagaosa, J. Phys. Spc. Jpn. **71**, 19 (2002).  
[6] T. Jungwirth *et al.*, Phys. Rev. Lett. **88**, 207208 (2002).  
[7] D. J. Thouless *et al.*, Phys. Rev. Lett. **49**, 405 (1982); M. Kohmoto, Ann. Phys. (N.Y.) **160**, 343 (1985).  
[8] M. Izumi *et al.*, J. Phys. Soc. Jpn. **66**, 3893 (1997); L. Klein *et al.*, Phys. Rev. B **61**, R7842 (2000); P. Matl *et al.*, Phys. Rev. B **57**, 10248 (1998); Y. Taguchi *et al.*, Science **291**, 2573 (2001).  
[9] *The Quantum Hall Effect*, edited by R. E. Prange and S. M. Girvin (Springer-Verlag, 1990).  
[10] D. N. Sheng *et al.*, Phys. Rev. B **64**, 165317 (2001); Y. Hatsugai *et al.*, Phys. Rev. Lett. **83**, 2246 (1999).  
[11] A. M. M. Pruisken in Ref. [9] and references therein.  
[12] F. D. M. Haldane, Phys. Rev. Lett. **61**, 2015 (1988).  
[13] A. MacKinnon and B. Kramer, Z. Phys. B **53**, 1 (1983).  
[14] E. Abrahams *et al.*, Phys. Rev. Lett. **42**, 673 (1979).  
[15] See the review article for the scaling theory of the IQHE B. Huckenstein, Rev. Mod. Phys. **67**, 357 (1995).

- [16] B. Huckenstein, *Europhys. Lett.* **20**, 451 (1992).
- [17] H. W. Jiang *et al.*, *Phys. Rev. Lett.* **71**, 1439 (1993).
- [18] M. A. Paalanen *et al.*, *Phys. Rev. B* **25**, 5566 (1982).
- [19] S. M. Girvin *et al.*, *Phys. Rev. B* **26**, 1651 (1982).
- [20] G. Bergmann and F. Ye, *Phys. Rev. Lett.* **67**, 735 (1991).
- [21] A. Langenfeld and P. Wölfle, *Phys. Rev. Lett.* **67**, 739 (1991).
- [22] J. P. Jan, *Helv. Phys. Acta.* **25**, 677 (1952).